JOURNAL OF COMPUTATIONAL PHYSICS 103, 222–230 (1992)

A Spectral Method for the Numerical Solutions of a Kinetic Equation Describing the Dispersion of Small Particles in a Turbulent Flow

TAO TANG* AND S. MCKEE

Department of Mathematics, University of Strathclyde, Glasgow G1 1XH, Scotland

AND

M. W. REEKS

Nuclear Electric plc., Berkeley Nuclear Laboratories, Berkeley, Gloucestershire GL13 9PB, England

Received September 19, 1990; revised October 11, 1991

In this paper we consider numerical solutions to a kinetic equation for the dispersion of small particles in a turbulent flow. The solution represents the probability density that a particle has a certain velocity and position at a given time. These solutions are based on a mixed finite-difference spectral method. Computational results are presented.

1. INTRODUCTION

Predicting the dispersion and deposition of small particles suspended in a turbulent flow is a problem of great practical importance both industrially and environmentally and has received considerable attention in the past (see, e.g., [1]). One of the authors (Reeks [2, 3]) recently derived a transport equation for the particle phase space probability density $w(\mathbf{v}, \mathbf{y}, t)$ for a particle with velocity $\mathbf{v}$ and position $\mathbf{y}$ at time t. This "kinetic" equation is in fact the analogue of the Maxwell–Boltzmann equation of classical kinetic theory (CKT); that is, it can be used in exactly the same way as the Maxwell–Boltzmann equation is used in CKT to construct the continuum equations and constitutive relations of the dispersed particle phase.

Finding a suitable kinetic equation hinges upon finding a suitable closed expression for the net acceleration of a particle resulting from its interaction with random turbulent eddies (inter-particle collisions are ignored). If the particle equation of motion is given by a Langevin equation then this is equivalent to finding a closed expression for the term $\langle W\mathbf{f} \rangle$, where $\mathbf{f}$ is the random fluctuating aerodynamic force, W is the instantaneous phase space density, and $\langle\ \rangle$ is a time or ensemble average. If $\mathbf{f}(t)$ is white noise, that is, its time scale is much shorter than that of particle motion, the kinetic equation reduces to the classical Fokker–Planck equation (see Chandrasekhar [4] and Buyevich [5, 6]) with

$$\langle W\mathbf{f} \rangle = -\boldsymbol{\mu}' \frac{\partial w}{\partial \mathbf{v}}, \tag{1.1}$$

where $\boldsymbol{\mu}'$ is a tensor whose components are in general functions of $\mathbf{y}$ and t with the diagonal components specifically positive. However, Reeks [2] was able to find a more general form for this "diffusion current" not restricted to white noise, by constructing expressions which preserved invariance to a random Galilean transformation (RGT) [7]. He showed that in general this term could be expressed as a series expansion involving successively higher order velocity and spatial derivatives of $w(\mathbf{v}, \mathbf{y}, t)$ and cumulants of $\mathbf{f}(t)$ along a particle trajectory. Significantly, truncation after the first term in the expansion corresponded to a realisable process in which $\mathbf{f}(t)$ is a Gaussian random process. In this case

$$\langle W\mathbf{f} \rangle = \left(\boldsymbol{\mu} \cdot \frac{\partial w}{\partial \mathbf{v}} + \boldsymbol{\lambda} \cdot \frac{\partial w}{\partial \mathbf{y}} \right), \tag{1.2}$$

where $\boldsymbol{\mu}$ and $\boldsymbol{\lambda}$ are tensors whose components are given functions of $\mathbf{y}$ and t. Using this form, the corresponding kinetic equation reproduces the correct equation of state [8] for the particle and preserves RGT invariance. Indeed the existence of the spatial gradient term can be traced directly to satisfying this latter requirement. For the case when $\mathbf{f}(t)$ is white noise the more general form reduces to that in Eq. (1.2) with $\boldsymbol{\lambda}$ effectively zero.

* Current address: Department of Mathematics and Statistics, Simon Fraser University, Burnaby, British Columbia, Canada V5A 1S6.

0021-9991/92 $5.00

We wish in this paper to consider ways of solving this kinetic equation for generic flows in which the dispersed phase is contained within some finite volume. Solutions of this sort will be particularly useful in several ways:

- in constructing constitutive relations;
- considering situations when simple gradient diffusion is inadequate, e.g., deposition of particles in turbulent boundary layers (see, e.g., [9]): in this case a solution can only be found by solving the kinetic equation explicitly;
- considering the influence of absorbing or partially reflecting boundaries: boundary conditions involving particles impacting and adhering at surfaces are in fact most naturally prescribed using this formulation (see, e.g., [2]).

As an illustration we consider here the one-dimensional form of the kinetic equation appropriate for dispersion of particles in inhomogeneous turbulence. For an axisymmetric pipe in which the mean carrier flow, $\bar{u}$, is uniform and axial (see Fig. 1) and in which the distribution of particles exhibits no spatial or velocity gradients in the axial direction the governing equation of the problem will be of the form (see [2])

$$\frac{\partial w}{\partial t} = -v\frac{\partial w}{\partial y} + \beta\frac{\partial (vw)}{\partial v} + \frac{\partial}{\partial v}\left[\mu\frac{\partial w}{\partial v} + \lambda\frac{\partial w}{\partial y}\right], \quad (1.3)$$

where μ and λ are given functions of y and t and β^{-1} is a constant representing the particle response time.

In this work, we shall consider Eq. (1.3) with simple Dirichlet boundary conditions:

$$w(-Y, v, t) = w_L(v, t), \qquad v \geqslant 0, t \geqslant 0; \quad (1.4)$$

$$w(Y, v, t) = w_R(v, t), \qquad v \leqslant 0, t \geqslant 0. \quad (1.5)$$

Initial conditions are given by

$$w(y, v, 0) = w_I(y, v), \qquad y \in (-Y, Y), \quad v \in (-\infty, +\infty). \quad (1.6)$$

Partial differential equations are often solved numerically by finite-difference methods (FDMs). Unfortunately, there are two main difficulties in solving (1.3)–(1.6) by FDMs.

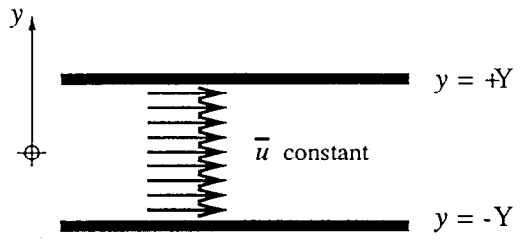

FIG. 1. The structure of a simple pipe flow.

First, due to the existence of the term $\partial^2 w/\partial v\,\partial y$ it is difficult to construct stable schemes for (1.3)–(1.6) (one can refer to [10–12] which consider FDMs for transport equations similar to (1.3) with $\lambda \equiv 0$, i.e., without the mixed term). Second, the eigenvalues of the resulting matrix arising from the discretised finite-difference schemes have different signs making it difficult to cope with the one sided boundary conditions (1.4) and (1.5). From the above, it would appear to be extremely difficult to construct proper FDMs to solve problem (1.3)–(1.6).

In recent years, there has been extensive activity in both the theory and application of spectral methods which have proved to be a powerful tool for obtaining numerical solutions of differential equations (see, e.g., [13–16]). In solving stationary neutron problems (similar to problem (1.3)–(1.6), but without the mixed term and in a finite domain), a method refered to as the "spherical harmonic method" has been used successfully (see, e.g., [17–20]). In this method the unknown function $w(y, v, t)$ ($|v| \leqslant 1$) is represented by an expansion of Legendre polynomials in v with coefficients depending on y and t. The method can be viewed as a certain type of spectral method for finite solution domain. When the problem is posed on $v \in (-\infty, \infty)$ (i.e., infinite domain) a variety of spectral techniques have been developed in recent years. These include the use of sine function, Hermite functions, and algebraically mapped Chebyshev polynomials and previous results for these techniques are summarized, for example, in Chapter 14 of Boyd [13]. Many researchers have noted that the close connection of Hermite polynomials to the physics makes them a natural choice of basis functions for many fields of science and engineering. Numerical applications include [21, 22] and many problems in tropical meteorology and oceanography (see also [23, 24]). In this paper we shall show that the spectral method with the use of the Hermite polynomials can produce very accurate numerical solutions for problem (1.3)–(1.6) in the infinite solution domain.

The remainder of the paper consists of three sections. Section 2 gives some series expansion results for the Hermite polynomials and Section 3 is devoted to the description of the spectral method used. The final section presents one numerical example for which the analytic solution is known. The numerical solutions of the problem using the spectral technique at various levels of truncation is compared with the analytic solution.

2. SERIES EXPANSION

Throughout this paper we shall assume that the given functions $\mu = \mu(y, t)$ and $\lambda = \lambda(y, t)$ are nonnegative and $\lambda(\pm Y, t) = 0$.

Since the solution interval of v in Eq. (1.3) is $(-\infty, +\infty)$ and the initial functions often assume the form

$\rho(y)\exp(-\alpha^2v^2)$, where $\rho(y)$ is a given nonnegative function and α is a positive constant, it is natural to represent the unknown function w by an expansion of the Hermite polynomials in v with coefficients depending on y and t. Substitution of this expansion into the kinetic equation (1.3) leads to simultaneous partial differential equations for the coefficients. Specifically, let

$$w(y, v, t)=\sum_{n=0}^{\infty}\frac{g_n(y, t)}{\sqrt{2^n n!}}f_n(y, t)\times H_n(\alpha v)\exp(-\alpha^2v^2), \tag{2.1}$$

where H_n is the nth order Hermite polynomial, g_n are given functions which are to be determined, and f_n are unknown functions. The extra factor $1/\sqrt{2^n n!}$ appearing in (2.1) will induce a symmetric coefficient matrix for the hyperbolic system for f_n (see (3.4)). Setting

$$\tilde{H}_n(v)=\frac{1}{\sqrt{2^n n!}}H_n(\alpha v)\exp(-\alpha^2v^2), \tag{2.2}$$

we have the following recurrence relations:

$$\frac{d\tilde{H}_n(v)}{dv}=-\alpha\sqrt{2(n+1)}\,\tilde{H}_{n+1}(v), \tag{2.3}$$

$$\frac{d^2\tilde{H}_n(v)}{dv^2}=\alpha^2\sqrt{4(n+1)(n+2)}\,\tilde{H}_{n+2}(v), \tag{2.4}$$

$$v\tilde{H}_n(v)=\frac{1}{\alpha}\left(\sqrt{\frac{n+1}{2}}\,\tilde{H}_{n+1}(v)+\sqrt{\frac{n}{2}}\,\tilde{H}_{n-1}(v)\right), \tag{2.5}$$

$$v\frac{d\tilde{H}_n(v)}{dv}=-\sqrt{(n+1)(n+2)}\,\tilde{H}_{n+2}(v)-(n+1)\,\tilde{H}_n(v). \tag{2.6}$$

From (2.1) and (2.5), we have

$$\begin{aligned}-v\frac{\partial w}{\partial y}=&-\sum_{n=0}^{\infty}\frac{1}{\alpha}\left[\sqrt{\frac{n+1}{2}}\,\tilde{H}_{n+1}(v)+\sqrt{\frac{n}{2}}\,\tilde{H}_{n-1}(v)\right]\\&\times\left[g_n(y, t)\frac{\partial f_n(y, t)}{\partial y}+\frac{\partial g_n(y, t)}{\partial y}f_n(y, t)\right]\\=&-\frac{1}{\alpha}\sum_{n=0}^{\infty}\left[\sqrt{\frac{n}{2}}\,g_{n-1}(y, t)\frac{\partial f_{n-1}(y, t)}{\partial y}\right.\\&\left.+\sqrt{\frac{n+1}{2}}\,g_{n+1}(y, t)\frac{\partial f_{n+1}(y, t)}{\partial y}\right]\tilde{H}_n(v)\\&-\frac{1}{\alpha}\sum_{n=0}^{\infty}\left[\sqrt{\frac{n}{2}}\,f_{n-1}(y, t)\frac{\partial g_{n-1}(y, t)}{\partial y}\right.\\&\left.+\sqrt{\frac{n+1}{2}}\,f_{n+1}(y, t)\frac{\partial g_{n+1}(y, t)}{\partial y}\right]\tilde{H}_n(v).\end{aligned} \tag{2.7}$$

Similarly, (2.1) and (2.6) yield

$$\frac{\partial}{\partial v}(vw)=-\sum_{n=0}^{\infty}\left[\sqrt{(n-1)n}\,g_{n-2}(y, t)f_{n-2}(y, t)+ng_n(y, t)f_n(y, t)\right]\tilde{H}_n(v). \tag{2.8}$$

From (2.1) and (2.4), we obtain

$$\mu\frac{\partial^2 w}{\partial v^2}=\alpha^2\mu\sum_{n=0}^{\infty}2\sqrt{(n-1)n}\,g_{n-2}(y, t)\times f_{n-2}(y, t)\,\tilde{H}_n(v); \tag{2.9}$$

and from (2.1) and (2.3), we have

$$\begin{aligned}\lambda\frac{\partial^2 w}{\partial v\,\partial y}=&-\lambda\sum_{n=0}^{\infty}\alpha\sqrt{2(n+1)}\,\tilde{H}_{n+1}(v)\\&\times\left[g_n(y, t)\frac{\partial f_n(y, t)}{\partial y}+\frac{\partial g_n(y, t)}{\partial y}f_n(y, t)\right]\\=&-\lambda\alpha\sum_{n=0}^{\infty}\left[\sqrt{2n}\,g_{n-1}(y, t)\frac{\partial f_{n-1}(y, t)}{\partial y}\right.\\&\left.+\sqrt{2n}\frac{\partial g_{n-1}(y, t)}{\partial y}f_{n-1}(y, t)\right]\tilde{H}_n(v).\end{aligned} \tag{2.10}$$

We now substitute (2.7)–(2.10) into Eq. (1.3) and equate the coefficient of $\tilde{H}_n(v)$ on the two sides of the equation. The result is a system of partial differential equations for the $f_n(y, t)$, which can be written in the form

$$\begin{aligned}g_n\frac{\partial f_n}{\partial t}+\frac{\partial g_n}{\partial t}f_n=&-\frac{1}{\alpha}\left[\sqrt{\frac{n+1}{2}}\,g_{n+1}\frac{\partial f_{n+1}}{\partial y}\right.\\&+\sqrt{\frac{n}{2}}\,g_{n-1}\frac{\partial f_{n-1}}{\partial y}+\sqrt{\frac{n+1}{2}}\frac{\partial g_{n+1}}{\partial y}f_{n+1}\\&\left.+\sqrt{\frac{n}{2}}\frac{\partial g_{n-1}}{\partial y}f_{n-1}\right]-n\beta g_n f_n+(2\alpha^2\mu-\beta)\\&\times\sqrt{(n-1)n}\,g_{n-2}f_{n-2}-\lambda\alpha\sqrt{2n}\\&\times\left[g_{n-1}\frac{\partial f_{n-1}}{\partial y}+\frac{\partial g_{n-1}}{\partial y}f_{n-1}\right].\end{aligned} \tag{2.11}$$

Equations (2.11) can be further re-arranged to give

$$\begin{aligned}\frac{\partial f_n}{\partial t}=&-\frac{1}{\alpha}\left[\sqrt{\frac{n+1}{2}}\frac{g_{n+1}}{g_n}\frac{\partial f_{n+1}}{\partial y}\right.\\&\left.+\sqrt{\frac{n}{2}}(1+2\lambda\alpha^2)\frac{g_{n-1}}{g_n}\frac{\partial f_{n-1}}{\partial y}\right]\\&+d_{n1}f_{n+1}+d_{n0}f_n+d_{n(-1)}f_{n-1}\\&+d_{n(-2)}f_{n-2},\end{aligned} \tag{2.12}$$

where

$$d_{n1} = -\frac{1}{\alpha}\sqrt{\frac{n+1}{2}}\frac{1}{g_n}\frac{\partial g_{n+1}}{\partial y}, \tag{2.13}$$

$$d_{n0} = -\left(n\beta + \frac{1}{g_n}\frac{\partial g_n}{\partial t}\right), \tag{2.14}$$

$$d_{n(-1)} = -\frac{1}{\alpha}\sqrt{\frac{n}{2}}\left[\frac{1}{g_n}\frac{\partial g_{n-1}}{\partial y} + 2\lambda\alpha^2\frac{1}{g_n}\frac{\partial g_{n-1}}{\partial y}\right], \tag{2.15}$$

$$d_{n(-2)} = (2\alpha^2\alpha - \beta)\sqrt{(n-1)n}\frac{g_{n-2}}{g_n}, \tag{2.16}$$

for $n = 0, 1, 2, \ldots$. Here the functions f_{-1} and f_{-2} have been set equal to 0.

Setting

$$g_n = g^{n/2} \qquad \text{with} \quad g = 1 + 2\lambda\alpha^2, \tag{2.17}$$

we obtain that

$$\frac{g_{n+1}}{g_n} = (1 + 2\lambda\alpha^2)\frac{g_{n-1}}{g_n} = \sqrt{g}. \tag{2.18}$$

Then Eqs. (2.12)–(2.16) become

$$\begin{aligned}\frac{\partial f_n}{\partial t} = &-\frac{\sqrt{g}}{\alpha}\left[\sqrt{\frac{n+1}{2}}\frac{\partial f_{n+1}}{\partial y} + \sqrt{\frac{n}{2}}\frac{\partial f_{n-1}}{\partial y}\right] \\ &+ d_{n1}f_{n+1} + d_{n0}f_n \\ &+ d_{n(-1)}f_{n-1} + d_{n(-2)}f_{n-2}.\end{aligned} \tag{2.19}$$

Further, using (2.12)–(2.16) and (2.19), we obtain

$$d_{n1} = -\frac{1}{\alpha}\left(\frac{n+1}{2}\right)^{3/2}\frac{1}{\sqrt{g}}\frac{\partial g}{\partial y}, \tag{2.20}$$

$$d_{n0} = -n\beta - \frac{n}{2g}\frac{\partial g}{\partial t}, \tag{2.21}$$

$$d_{n(-1)} = -\frac{n-1}{2\alpha}\sqrt{\frac{n}{2g}}\frac{\partial g}{\partial y}, \tag{2.22}$$

$$d_{n(-2)} = (2\alpha^2\mu - \beta)\sqrt{(n-1)n}/g, \tag{2.23}$$

for $n = 0, 1, 2, \ldots$.

3. SPECTRAL METHOD

The spectral method of order N is the result of solving the first $N+1$ of the Eqs. (2.19) for the $N+1$ unknown functions $f_0, f_1, \ldots$, after f_{N+1} has been set equal to 0 in the last of these equations. The spectral approximation to $w(y, v, t)$ will be given by

$$w_N(y, v, t) = \sum_{n=0}^{N}\frac{g_n(y, t)}{\sqrt{2^n n!}}f_n(y, t) \times H_n(\alpha v)\exp(-\alpha^2 v^2). \tag{3.1}$$

Let $\mathbf{F}$ denote an $(N+1)$-dimensional column vector defined by

$$\mathbf{F} = \mathbf{F}(y, t) = [f_0(y, t), f_1(y, t), \ldots, f_N(y, t)]^{\mathrm{T}}. \tag{3.2}$$

Then Eqs. (2.19) become

$$\frac{\partial \mathbf{F}}{\partial t} = -\frac{\sqrt{g}}{\alpha}\mathbf{R}\frac{\partial \mathbf{F}}{\partial y} + \mathbf{S}\mathbf{F}, \tag{3.3}$$

where $\mathbf{R}$ and $\mathbf{S}$ are $(N+1)\times(N+1)$ matrices given by

$$\mathbf{R} = \begin{pmatrix} 0 & \sqrt{\frac{1}{2}} & 0 & 0 & 0 & \cdots \\ \sqrt{\frac{1}{2}} & 0 & \sqrt{\frac{2}{2}} & 0 & 0 & \cdots \\ 0 & \sqrt{\frac{2}{2}} & 0 & \sqrt{\frac{3}{2}} & 0 & \cdots \\ 0 & 0 & \sqrt{\frac{3}{2}} & 0 & \sqrt{\frac{4}{2}} & \cdots \\ \vdots & \vdots & \ddots & \ddots & \ddots & \vdots \end{pmatrix}, \tag{3.4}$$

and

$$\mathbf{S} = \begin{pmatrix} d_{00} & d_{01} & 0 & 0 & 0 & 0 & \cdots \\ d_{1(-1)} & d_{10} & d_{11} & 0 & 0 & 0 & \cdots \\ d_{2(-2)} & d_{2(-1)} & d_{20} & d_{21} & 0 & 0 & \cdots \\ 0 & d_{3(-2)} & d_{3(-1)} & d_{30} & d_{31} & 0 & \cdots \\ \vdots & \ddots & \ddots & \ddots & \ddots & \ddots & \vdots \end{pmatrix}. \tag{3.5}$$

It can be seen from (3.4) that the matrix $\mathbf{R}$ is symmetric and thus has real eigenvalues. Specifically, we have the following result.

THEOREM 1. *The eigenvalues of* $\mathbf{R}$ *are the zeros of the Hermite polynomial* $H_{N+1}(\gamma)$.

Proof. Let $\mathfrak{R}_{N+1}(\gamma) = \det(\gamma I - \mathbf{R})$. Expanding the determinant about its last row results in two terms, arising from the last two elements of that row, we then obtain

$$\mathfrak{R}_{N+1}(\gamma) = \gamma\mathfrak{R}_N(\gamma) - \frac{N}{2}\mathfrak{R}_{N-1}(\gamma). \tag{3.6}$$

We shall prove that

$$\mathfrak{R}_N(\gamma) = 2^{-N}H_N(\gamma), \qquad N \geqslant 1. \tag{3.7}$$

This can be verified for $N=1$ and 2 by direct calculations. If (3.7) holds for $N \leqslant L$, we have, by using (3.6), that

$$\begin{aligned}\mathfrak{R}_{L+1}(\gamma) &= \gamma \mathfrak{R}_L(\gamma) - \frac{L}{2}\mathfrak{R}_{L-1}(\gamma) \\ &= 2^{-L}\gamma H_L(\gamma) - 2^{-L} L H_{L-1}(\gamma) \\ &= 2^{-(L+1)}(2\gamma H_L(\gamma) - 2L H_{L-1}(\gamma)) \\ &= 2^{-(L+1)} H_{L+1}(\gamma). \end{aligned} \tag{3.8}$$

This completes the proof of Theorem 1. ∎

Let $\gamma_0 > \gamma_1 > \cdots > \gamma_N$ be the zeros of the Hermite polynomial $H_{N+1}(\gamma)$; and set

$$C_k = \left\{ \sum_{n=0}^{N} \frac{1}{2^n n!} [H_n(\gamma_k)]^2 \right\}^{-1}. \tag{3.9}$$

We have the following results concerning the eigenvectors of $\mathbf{R}$.

THEOREM 2. (i) *The eigenvector of* $\mathbf{R}$ *corresponding to the eigenvalue* γ_k *is*

$$U_k = [U_{0k}, U_{1k}, ..., U_{nk}]^{\mathrm{T}}, \tag{3.10}$$

with

$$U_{nk} = \frac{C_k}{\sqrt{2^n n!}} H_n(\gamma_k). \tag{3.11}$$

(ii) *The element of the inverse matrix of* $U \equiv [U_0, U_1, ..., U_N]$ *is of the form*

$$(U^{-1})_{nk} = \frac{1}{\sqrt{2^k k!}} H_k(\gamma_n). \tag{3.12}$$

Proof. (i) If $\mathbf{R}Y = \gamma_k Y$, then

$$\sqrt{\frac{n}{2}}\, y_{n-1} + \sqrt{\frac{n+1}{2}}\, y_{n+1} = \gamma_k y_n, \tag{3.13}$$

for $n = 0, 1, ..., N$; and y_{-1}, y_{N+1} are set equal to 0. It is straightforward to show that the recurrence relation (3.13) is satisfied by $y_n = U_{nk}$, where U_{nk} is defined by (3.11).

(ii) Since the corresponding eigenvectors U_i and U_j of two different eigenvalues γ_i and γ_j are mutually orthogonal, we have

$$\sum_{n=0}^{N} \frac{1}{2^n n!} H_n(\gamma_i) H_n(\gamma_j) = C_j \delta_{ij}, \tag{3.14}$$

which implies that $(U^{-1})_{nk} = H_k(\gamma_n)/\sqrt{2^k k!}$. The proof of Theorem 2 is therefore complete. ∎

Let $\tilde{F} = U^{-1}F$ and $\tilde{S} = U^{-1}SU$. From Theorem 2 we obtain that

$$U^{-1}\mathbf{R}U = \Lambda \equiv \mathrm{diag}(\gamma_0, \gamma_1, ..., \gamma_N). \tag{3.15}$$

If we premultiply (3.3) by U^{-1}, we obtain

$$\frac{\partial \tilde{F}}{\partial t} = -\frac{\sqrt{g}}{\alpha}\Lambda \frac{\partial \tilde{F}}{\partial y} + \tilde{S}\tilde{F}. \tag{3.16}$$

Since the function g is positive, Eq. (3.16) is a typical hyperbolic system and can be solved by forward and backward space differences according to the signs of γ_k $(0 \leqslant k \leqslant N)$. The boundary conditions for $\tilde{F}$ are, when N is odd,

$$\tilde{f}_j(-Y, t) = w_{\mathrm{L}}(\gamma_j/\alpha, t)\exp(\gamma_j^2), \quad j = 0, 1, ..., \frac{N-1}{2}, \tag{3.17}$$

$$\tilde{f}_j(Y, t) = w_{\mathrm{R}}(\gamma_j/\alpha, t)\exp(\gamma_j^2), \quad j = \frac{N+1}{2}, ..., N. \tag{3.18}$$

If N is even, then $\gamma_{N/2} = 0$. In this case the system of Eqs. (3.16) for $\tilde{f}_{N/2}(y, t)$ needs no boundary condition because $\partial/\partial y$ does not appear. Hence in this case

$$\tilde{f}_j(-Y, t) = w_{\mathrm{L}}(\gamma_j/\alpha, t)\exp(\gamma_j^2), \quad j = 0, 1, ..., \frac{N}{2} - 1, \tag{3.19}$$

$$\tilde{f}_j(Y, t) = w_{\mathrm{R}}(\gamma_j/\alpha, t)\exp(\gamma_j^2), \quad j = \frac{N}{2} + 1, ..., N. \tag{3.20}$$

To derive the above boundary conditions, we may write from (2.1) that

$$w(y, \gamma_j/\alpha, t) \approx w_N(y, \gamma_j/\alpha, t) = \sum_{n=0}^{N} \frac{g_n(y, t)}{\sqrt{2^n n!}} \times f_n(y, t)\, H_n(\gamma_j)\exp(-\gamma_j^2). \tag{3.21}$$

From (2.17), together with $\lambda(\pm Y, t) = 0$, we have $g_n(\pm Y, t) = 1$. This and (3.21) yield that

$$w(\pm Y, \gamma_j/\alpha, t) \approx \tilde{f}_j(\pm Y, t)\exp(-\gamma_j^2). \tag{3.22}$$

When N is odd, $\gamma_j > 0$ when $j \leqslant (N-1)/2$ and $\gamma_j < 0$ when $j \geqslant (N+1)/2$. From (1.4), (1.5), and (3.22), we choose the boundary conditions (3.17)–(3.18). The boundary conditions (3.19)–(3.20) are obtained in a similar way.

4. NUMERICAL EXAMPLES

Consider the test problem

$$\frac{\partial w}{\partial t} = -v\frac{\partial w}{\partial y} + \frac{\partial (vw)}{\partial v} + \frac{\partial^2 w}{\partial v^2}, \tag{4.1}$$

$$w(-1, v, t) = \frac{1}{2}\left[1 - \sin\left(\frac{\pi}{2}(1-e^{-t})v\right) q(t)\right] \times \exp\left(-\frac{v^2}{2}\right), \qquad v \geqslant 0, \tag{4.2}$$

$$w(1, v, t) = \frac{1}{2}\left[1 + \sin\left(\frac{\pi}{2}(1-e^{-t})v\right) q(t)\right] \times \exp\left(-\frac{v^2}{2}\right), \qquad v \leqslant 0, \tag{4.3}$$

$$w(y, v, 0) = \frac{1}{2}\left(1 + \cos\frac{\pi y}{2}\right)\exp\left(-\frac{v^2}{2}\right), \tag{4.4}$$

with

$$q(t) = \exp\left[-\frac{\pi^2}{4}\left(t + 2e^{-t} - \frac{1}{2}e^{-2t} - \frac{3}{2}\right)\right].$$

The exact solution of (4.1)–(4.4) is

$$w(y, v, t) = \frac{1}{2}\left[1 + \cos\left(\frac{\pi}{2}(y - (1-e^{-t})v)\right) q(t)\right] \times \exp\left(-\frac{v^2}{2}\right). \tag{4.5}$$

Problem (4.1)–(4.4) has been chosen since it has an analytic solution and this allows us to compare our numerical results with the exact solution (4.5). It is noted that the analytic solution satisfies $0 \leqslant w(y, v, t) \leqslant 1$ which indicates that the test problem (4.1)–(4.4) is more realistic than that given in [25], where the test problem does not lead to a positive semidefinite solution.

In the following numerical calculations, several values of N (see (3.2) for N) are tested. We use $N = 2, 3, 4, 6$, and 8, respectively, which correspond to 3, 4, 5, 7, and 9 truncated terms in the series expansion (2.1). The constant α (see (2.1)) used in the calculations is $1/\sqrt{2}$. The Hermite polynomials $H_{N+1}(\gamma)$, for $N = 2, 3, 4, 6$, and 8, are

$$H_3(\gamma) = 8\gamma^3 - 12\gamma, \tag{4.6}$$

$$H_4(\gamma) = 16\gamma^4 - 48\gamma^2 + 12, \tag{4.7}$$

$$H_5(\gamma) = 32\gamma^5 - 160\gamma^3 + 120\gamma, \tag{4.8}$$

$$H_7(\gamma) = 128\gamma^7 - 1344\gamma^5 + 3360\gamma^3 - 1680\gamma, \tag{4.9}$$

$$H_9(\gamma) = 512\gamma^9 - 9216\gamma^7 + 48384\gamma^5 - 80640\gamma^3 + 30240\gamma. \tag{4.10}$$

The roots of the above polynomials, which in general cannot be found analytically for large N, are obtained numerically. They are

$$H_3: 1.2247, 0, -1.2247; \tag{4.11}$$

$$H_4: 1.6507, 0.5246, -0.5246, -1.6507; \tag{4.12}$$

$$H_5: 2.0202, 0.9586, 0, -0.9586, -2.0202; \tag{4.13}$$

$$H_7: 2.6520, 1.6735, 0.8163, 0, -0.8163, -1.6735, -2.6520; \tag{4.14}$$

$$H_9: 3.1910, 2.2666, 1.4685, 0.7235, 0, -0.7235, -1.4685, -2.2666, -3.1910. \tag{4.15}$$

Using (4.6)–(4.15) we can find the corresponding matrices U and U^{-1}. The finite-difference scheme for (3.16), for $0 \leqslant j \leqslant N$, is

$$\tilde{f}_j(y, t+\Delta t) = \tilde{f}_j(y, t) - \frac{\gamma_j}{\alpha}\frac{\Delta t}{\Delta y} g^{1/2}(y, t) \times (\tilde{f}_j(y, t) - \tilde{f}_j(y - \Delta y, t)) + \Delta t(\tilde{S}\tilde{F})_j(y, t), \qquad \text{if} \quad \gamma_j > 0; \tag{4.16}$$

$$\tilde{f}_j(y, t+\Delta t) = \tilde{f}_j(y, t) - \frac{\gamma_j}{\alpha}\frac{\Delta t}{\Delta y} g^{1/2}(y, t) \times (\tilde{f}_j(y + \Delta y, t) - \tilde{f}_j(y, t)) + \Delta t(\tilde{S}\tilde{F})_j(y, t), \qquad \text{if} \quad \gamma_j < 0; \tag{4.17}$$

and

$$\tilde{f}_j(y, t+\Delta t) = \tilde{f}_j(y, t) + \Delta t(\tilde{S}\tilde{F})_j(y, t), \qquad \text{if} \quad \gamma_j = 0. \tag{4.18}$$

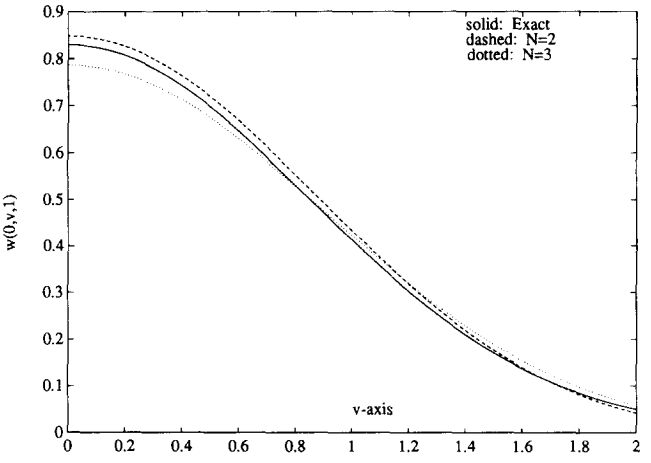

FIG. 2. The variation of $w(0, v, t)$ with $0 \leqslant v \leqslant 2$ at $t = 1$. The numerical results are obtained by using three and four truncated terms (i.e., $N = 2$ and 3).

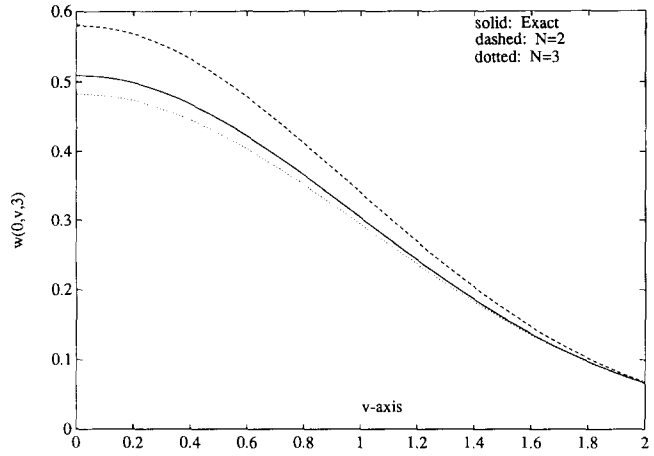

FIG. 3. The variation of $w(0, v, t)$ with $0 \leqslant v \leqslant 2$ at $t = 3$. The numerical results are obtained by using 3 and 4 truncated terms (i.e., $N = 2$ and 3).

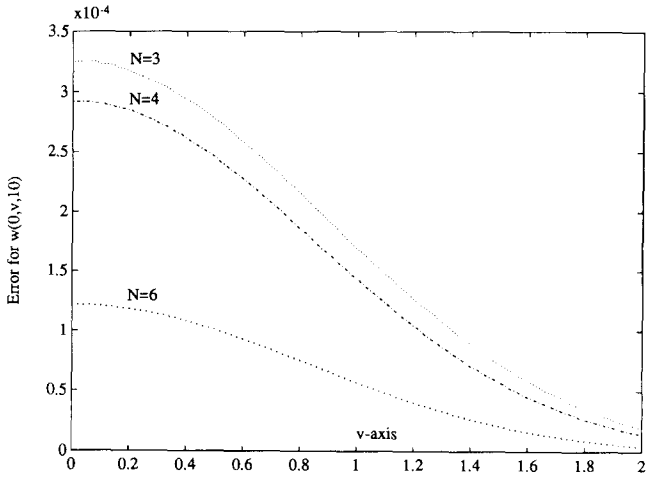

FIG. 5. The variation of $|w(0, v, 10) - w_N(0, v, 10)|$ for $N = 3$, 4, and 6.

Here Δt and Δy are steplengths in t and y directions, respectively. Equations (4.16) and (4.17) are solved with the boundary conditions (3.17)–(3.18) (if N is odd) or (3.19)–(3.20) (if N is even). The stability restriction, i.e., Courant–Friedrichs–Lewy condition,

$$\frac{\Delta t}{\Delta y} \max_{0 \leqslant j \leqslant N} |\gamma_j| \leqslant 1, \tag{4.19}$$

must be satisfied. In the present calculations the mesh sizes used are $\Delta y = 0.02$ and $\Delta t = 0.001$. Since the maximum eigenvalue used in our calculations is 3.191 (see (4.15)) the above CFL condition is satisfied.

In order to compare numerical and theoretical solutions of (4.1)–(4.4), we plot $w(0, v, t)$ for $0 \leqslant v \leqslant 2$ at different time levels. Figure 2 shows numerical results of $w(0, v, 1)$ obtained by the use of three and four truncated terms (i.e., $N = 2$ and $N = 3$). The theoretical solutions given by (4.5) are also plotted in Fig. 2. It is observed that the agreement between the numerical and theoretical results is favourable. However, as t grows the agreement between the theoretical solution and the numerical result obtained by using three truncated terms (i.e., $N = 2$) breaks down. This can be seen from Fig. 3 which plots $w(0, v, 3)$, obtained by using $N = 2$ and $N = 3$, respectively. Figure 3 suggests that $N = 2$ is too small to obtain accurate numerical solutions.

Figure 4 gives the theoretical and numerical results of $w(0, v, 5)$. The numerical results presented in Fig. 4 are obtained by using four and five truncated terms (i.e., $N = 3$ and 4). It can be observed from Fig. 4 that the numerical solution with $N = 3$ and 4 at $t = 5$ compares very well with the theoretical one. As time t becomes sufficiently large the solution of problem (4.1)–(4.2) reaches a steady state, i.e.,

$$w(y, v, t) \sim \exp\left(-\frac{v^2}{2}\right). \tag{4.20}$$

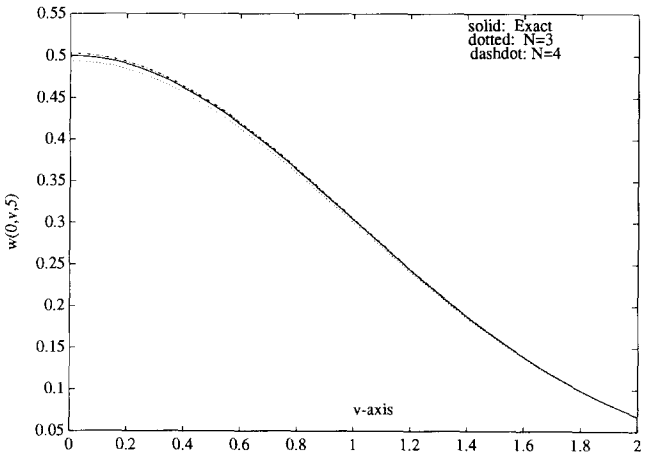

FIG. 4. The variation of $w(0, v, t)$ with $0 \leqslant v \leqslant 2$ at $t = 5$. The numerical results are obtained by using 4 and 5 truncated terms (i.e., $N = 3$ and 4).

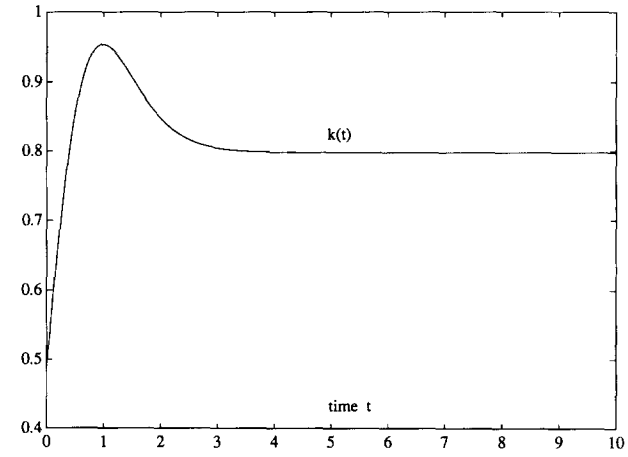

FIG. 6. The variation of $k(t)$ with $0 \leqslant t \leqslant 10$.

The spectral solutions approximate this steady state solution very well, but it is difficult to plot them so that they are distinguishable from the exact solution. Instead, Fig. 5 shows the numerical errors $|w(0, v, 10) - w_N(0, v, 10)|$, with $N = 3$, 4, and 6, which are observed to be of order $O(10^{-4})$.

In practice, we require, in particular, the so-called current to the wall k, defined as

$$k(t) = \frac{(\int_0^{+\infty} vw(Y, v, t)\, dv)}{((1/2Y)\int_{-Y}^{Y}\int_0^{+\infty} w(y, v, t)\, dv\, dy)}. \tag{4.21}$$

For problem (4.1)–(4.4), a direct calculation from (4.5) and (4.21) gives (see Fig. 6)

$$k(t) = \frac{\begin{pmatrix} 1 + (\pi/2)(1 - e^{-t})\, q(t) \\ \quad \times \int_0^{\infty} \cos((\pi/2)(1 - e^{-t})v) \exp(-(v^2/2))\, dv \end{pmatrix}}{\begin{pmatrix} \sqrt{\pi/2} + (2/\pi)\, q(t) \\ \quad \times \int_0^{\infty} \cos((\pi/2)(1 - e^{-t})v) \exp(-(v^2/2))\, dv \end{pmatrix}}. \tag{4.22}$$

On the other hand, using

$$\text{(i)} \quad \int_0^{\infty} H_n(\alpha v) \exp(-\alpha^2 v^2)\, dv = \begin{cases} \sqrt{\pi}/2\alpha & n = 0 \\ H_{n-1}(0)/\alpha, & n \geqslant 1, \end{cases} \tag{4.23}$$

and

$$\text{(ii)} \quad \int_0^{\infty} vH_n(\alpha v) \exp(-\alpha^2 v^2)\, dv = \begin{cases} 1/2\alpha^2, & n = 0, \\ \sqrt{\pi}/2\alpha^2, & n = 1, \\ H_{n-2}(0)/\alpha^2, & n \geqslant 2, \end{cases} \tag{4.24}$$

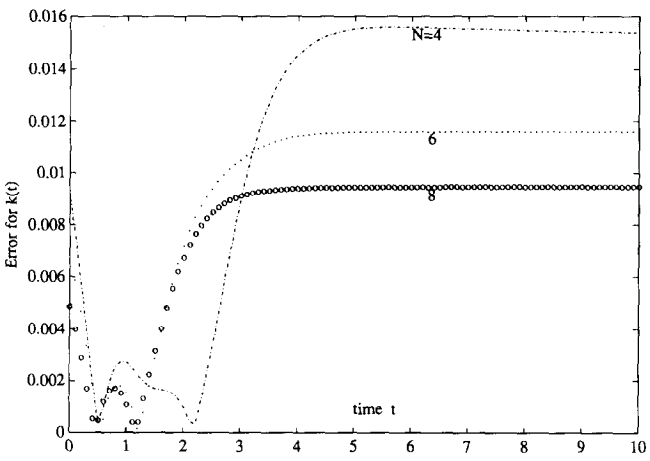

FIG. 7. The variation of $|k(t) - k_N(t)|$ for $N = 4$, 6, and 8.

we obtain from (3.1) and (4.21) that

$$k(t) \approx k_N(t) = \frac{1}{\alpha} \frac{\begin{pmatrix} f_0(Y, t) + \sqrt{\pi/2} f_1(Y, t) \\ \quad + \sum_{n=2}^{N} 2f_n(Y, t)\, H_{n-2}(0)/\sqrt{2^n n!} \end{pmatrix}}{\begin{pmatrix} \sqrt{\pi/2} \int_{-1}^{1} f_0(y, t)\, dy \\ \quad + \sum_{n=1}^{N} H_{n-1}(0) \int_{-1}^{1} f_n(y, t)\, dy/\sqrt{2^n n!} \end{pmatrix}}. \tag{4.25}$$

Figure 7 shows the numerical errors $|k(t) - k_N(t)|$ for $N = 4$, 6, and 8. It is observed that the calculated solutions of k are in good agreement with the theoretical results when larger values of N are employed. Physically, we also need to predict the long-time behavior of $k(t)$. In other words, $k(\infty)$ is of practical importance in the investigations. The present numerical calculation of k_8 suggests that $k_8(\infty) = 0.807$, yielding a relative error with respect to $k(\infty)(= \sqrt{2/\pi})$ of

$$\frac{k_8(\infty) - k(\infty)}{k(\infty)} \approx 1\%. \tag{4.26}$$

ACKNOWLEDGMENTS

We are grateful to Keith Hyland, David Swailes, and the referees for many helpful comments and suggestions which have improved the presentation and content of this paper.

REFERENCES

1. C. T. Crowe, *J. Fluids Eng.* **104**, 297 (1982).
2. M. W. Reeks, *Phys. Fluids A* **3**, 446 (1991).
3. M. W. Reeks, *On the Continuum Equations for Dispersed Particles in Non-uniform Flows, Phys. Fluids A*, to appear.
4. S. Chandrasekhar, *Rev. Mod. Phys.* **15**, 1 (1943).
5. Y. A. Buyevich, *J. Fluid. Mech.* **49**, 489 (1971).
6. Yu. A. Buyevich, *J. Fluid Mech.* **52**, 345 (1972).
7. R. H. Kraichnan, *J. Fluid Mech.* **83**, 349 (1977).
8. M. W. Reeks, in *Symposium on Gas-Solid Flows*, New Orleans (ASME, New York, 1984), p. 9.
9. M. W. Reeks, *J. Aerosol Sci.* **14**, 729 (1983).
10. B. G. Carlson, *The S_n Method*, Los Alamos report and subsequent reports, 1953 (unpublished).
11. K. O. Friedrichs, *Commun. Pure Appl. Math.* **7**, 345 (1954).
12. H. B. Keller and B. Wendroff, *Commun. Pure Appl. Math.* **10**, 567 (1957).
13. J. P. Boyd, *Chebyshev and Fourier Spectral Methods* (Springer-Verlag, Berlin/Heidelberg, 1989).
14. C. Canuto, M. Y. Hussaini, A. Quarteroni, and T. A. Zang, *Spectral Methods in Fluid Mechanics* (Springer-Verlag, Berlin/Heidelberg, 1988).

15. D. Gottlieb and S. Orszag, *Numerical Analysis of Spectral Methods: Theory and Applications*, CBMS-NSF Regional Conference Series in Applied Mathematics, Vol. 26 (SIAM, Philadelphia, 1977).
16. C. Ringhofer, *SIAM J. Numer. Anal.* **27**, 32 (1990).
17. S. Chandrasekhar, *Astrophys. J.* **99**, 180 (1944).
18. S. Chandrasekhar, *Astrophys. J.* **100**, 82 (1944).
19. R. D. Richtmyer and K. W. Morton, *Difference Methods for Initial-Value Problems*, 2nd ed. (Interscience, New York, 1967).
20. G. C. Wick, *Z. Phys.* **121**, 702 (1943).
21. K. Banerjee, *Proc. Roy. Soc. London A* **364**, 264 (1978).
22. G. Birkhoff and G. Fix, in *Numerical Solution of Field Problems in Continuum Mechanics*, Vol. 2 SIAM-AMS Proceedings (Amer. Math. Soc., Providence, RI, 1970), p. 111.
23. J. P. Boyd and D. W. Moore, *Dyn. Atmos. Sci.* **10**, 51 (1986).
24. H. G. Marshall and J. P. Boyd, *J. Phys. Oceanogr.* **17**, 1016 (1987).
25. M. W. Reeks, T. Tang, K. Hyland, S. McKee and D. Swailes, in *Symposium on Gas-Solid Flows, Oregon*, (ASME, New York, 1991), p. 45.